

Confirmation of sulfur tolerance of bimetallic Pd–Pt supported on highly acidic USY zeolite by EXAFS

Hiroyuki Yasuda*, Nobuyuki Matsubayashi, Toshio Sato and Yuji Yoshimura

National Institute of Materials and Chemical Research, Tsukuba, Ibaraki 305-8565, Japan

E-mail: yasuda@nimc.go.jp

Received 25 March 1998; accepted 19 June 1998

The sulfur tolerance (i.e., degree of sulfidation) of Pd and Pt in sulfided bimetallic Pd–Pt catalysts (Pd:Pt mole ratio of 4:1) supported on USY (ultrastable Y) zeolites ($\text{SiO}_2/\text{Al}_2\text{O}_3 = 10.7, 48, \text{ and } 310$) was investigated using an extended X-ray absorption fine structure (EXAFS) method. The sulfidation of the catalysts was done in a 1000 ppm H_2S –2% H_2/N_2 stream at 573 K for 0.5 h. In the Fourier transforms of Pd K-edge and Pt L_{III}-edge EXAFS spectra, both of the peaks due to metallic Pd and to metallic Pt for the Pd–Pt/USY ($\text{SiO}_2/\text{Al}_2\text{O}_3 = 10.7$) catalyst remained most after sulfidation. Further, the results of the Fourier transforms confirmed that the sulfur tolerance of both Pd and Pt decreased with increasing $\text{SiO}_2/\text{Al}_2\text{O}_3$ ratio, suggesting that Pd and Pt become sulfur-tolerant when Pd–Pt bimetallic particles are supported on highly acidic USY zeolite.

Keywords: EXAFS, sulfided bimetallic catalysts, Pd, Pt, USY zeolites, sulfur tolerance

1. Introduction

Recently, for deep hydrogenation of aromatics in diesel fuel, much attention has been paid to highly sulfur-tolerant Pd–Pt bimetallic catalysts [1,2]. The catalytic performances of bimetallic Pd–Pt on various supports, such as Al_2O_3 and acidic zeolites, have been reported [3–8]. For the hydrogenation of tetralin in the presence of dibenzothiophene, we previously investigated the influence of the acidity of the supports on the activity of Pd–Pt catalysts by using HY and USY (ultrastable Y) zeolites in which the $\text{SiO}_2/\text{Al}_2\text{O}_3$ ratio was widely varied from 5.6 to 680. The results showed that both the activity and the sulfur tolerance strongly depend on the $\text{SiO}_2/\text{Al}_2\text{O}_3$ ratio: the activity first increases with an increase in the ratio, reaches a maximum when the ratio is in the 15 to 40 range, and then gradually decreases as the ratio further increases to 680 [9]. The hydrogenation activity of these catalysts was thought to be related to the ease of the diffusion of the reactant into zeolite micropores as well as to the sulfur tolerance of supported noble metals. However, there is currently no definitive evidence for the effect of the acidity ($\text{SiO}_2/\text{Al}_2\text{O}_3$ ratio) of USY zeolites on the sulfur tolerance of noble metals on USY.

Extended X-ray absorption fine structure (EXAFS) is a suitable method for the investigation on the local structures and the sulfidation states of Pd and Pt for Pd–Pt/USY catalysts. Based on EXAFS analyses, several researchers have proposed structures of bimetallic Pd–Pt fine particles [10–12]. However, little is known about the changes in the Pd–Pt metals after sulfidation [13].

In the present study, we prepared three kinds of Pd–Pt/USY catalysts with different $\text{SiO}_2/\text{Al}_2\text{O}_3$ ratios, and then

attempted to elucidate the influence of the acidity of the supports on the sulfur tolerance of Pd–Pt by investigating the degree of sulfidation for both Pd and Pt for sulfided Pd–Pt/USY catalysts by using an EXAFS technique.

2. Experimental

2.1. Preparation and characterization of Pd–Pt/USY catalysts

Three kinds of USY zeolites having different $\text{SiO}_2/\text{Al}_2\text{O}_3$ ratios were used as supports: USY ($\text{SiO}_2/\text{Al}_2\text{O}_3 = 10.7$), designated as USY-10.7) was obtained from Tosoh Co. and used as received. USY with $\text{SiO}_2/\text{Al}_2\text{O}_3 = 47.5$ (designated as USY-48) was prepared by treating USY (Tosoh Co.; $\text{SiO}_2/\text{Al}_2\text{O}_3 = 13.9$) with hydrochloric acid (0.05 mol dm^{−3}) at 298 K for 24 h. After the treatment, the dealuminated zeolite was filtered, washed with water until no chloride ions were detected in the fresh filtrate, and then dried at 383 K overnight. USY with $\text{SiO}_2/\text{Al}_2\text{O}_3 = 307$ (designated as USY-310) was prepared in the same manner except the hydrochloric acid concentration was 2.0 mol dm^{−3}, the treatment temperature was 373 K, and the treatment time was 2 h. The $\text{SiO}_2/\text{Al}_2\text{O}_3$ ratios of USY-48 and USY-310 were determined using an ICP spectrometer (Seiko Instruments, SPS1200A).

The bimetallic Pd–Pt catalysts supported on USY-10.7, USY-48, and USY-310 were prepared by incipient wetness impregnation with a mixed aqueous solution of $[\text{Pd}(\text{NH}_3)_4]\text{Cl}_2$ and $[\text{Pt}(\text{NH}_3)_4]\text{Cl}_2$. For a reference catalyst, we prepared a Pd–Pt catalyst supported on $\gamma\text{-Al}_2\text{O}_3$ (Catalyst and Chemical Industries Co.; SA, 200 m² g^{−1}; PV, 0.8 cm³ g^{−1}). The total metal content of each catalyst

* To whom correspondence should be addressed.

was 1.2 wt%, and the mole ratio of Pd to Pt was 4. The impregnated samples were dried in vacuum at 333 K for 6 h, and calcined in an O₂ stream (2 dm³ min^{−1} g^{−1}) at 573 K for 3 h at a heating rate of 0.5 K min^{−1}.

Metal dispersions of the Pd–Pt/USY catalysts were determined from the amount of chemisorbed CO measured with a pulse method. Prior to the chemisorption measurement, the precalcined sample (ca. 50 mg) was reduced in an H₂ stream (30 cm³ min^{−1}) at 573 K for 1 h and then purged by He at the same temperature for 10 min. Pulses (0.5 cm³) of 9.8% CO (in He) were injected into a stream of He carrier gas (30 cm³ min^{−1}) and contacted with the catalyst at room temperature. The amount of chemisorbed CO was analyzed by a thermal conductivity detector. In the calculation of the dispersion, the stoichiometry of CO to either Pd or Pt was assumed to be unity. The average metal particle size was estimated using the equation $d = 5/\rho S$ (d , metal particle size; ρ , density of the metal; S , surface area of the metal), assuming that both Pd and Pt atoms were exposed to the surface at the atomic ratio of 4:1. The cross-sectional areas of Pd and Pt were assumed to be 0.0787 and 0.0800 nm², respectively [14].

2.2. EXAFS measurement

The EXAFS spectra of Pd K-edge (24.3 keV) and Pt L_{III}-edge (11.6 keV) for sulfided Pd–Pt/USY and Pd–Pt/ γ -Al₂O₃ catalysts were measured using a Si(311) double-crystal monochromator at the Photon Factory (BL-10B) of the Institute of Materials Structure Science (KEK-PF in Tsukuba, Japan). All measurements were done at room temperature using an EXAFS cell (cell volume of about 1.0 cm³) that had an optical path length of 8–15 mm and polyimide film windows.

The precalcined sample (180 mg for the Pt L_{III}-edge measurement and 280 mg for the Pd K-edge measurement) was first reduced in an H₂ stream (100 cm³ min^{−1}) at 573 K for 3 h in a Pyrex tube that had vacuum cocks and the cell, then sulfided in a 1000 ppm H₂S–2% H₂ (in N₂) stream (100 cm³ min^{−1}) at 573 K for 0.5 h, and then finally cooled to room temperature in the same H₂S–H₂ atmosphere. After this treatment, the cocks were closed to avoid contamination of the sample by air. The sample was then transferred into the connected cell, evacuated for 3 min, and sealed under vacuum (10^{−3} Torr). For references, we used PdO, PtO₂, Pd-foil, and Pt-foil. The thickness of the Pd- and Pt-foils was about 16 and 5 μ m, respectively.

EXAFS spectra were extracted from X-ray absorption spectra using a cubic spline function. Fourier transformation of the k^3 -weighted EXAFS data was done in the Δk range of 14 \AA^{-1} for Pd K-edge and in the 13 \AA^{-1} for Pt L_{III}-edge with a square window dumping at 5% at either side of the range by a Hamming function. The error in the radial distance R was estimated from repeated measurements to be ± 0.01 \AA .

Table 1
Metal dispersion and average metal particle size of Pd–Pt/USY catalysts.

| Catalyst ^a | Metal dispersion (%) | Average metal particle size (\AA) |
|-----------------------|----------------------|--|
| Pd–Pt/USY-10.7 | 37 | 25 |
| Pd–Pt/USY-48 | 35 | 27 |
| Pd–Pt/USY-310 | 30 | 31 |

^a Metal contents of Pd and Pt were 0.9 and 0.3 wt%, respectively.

3. Results and discussion

Table 1 summarizes the metal dispersion and the average metal particle size of Pd–Pt/USY catalysts. The metal dispersion was the highest for Pd–Pt/USY-10.7 (37%), and slightly decreased with increasing SiO₂/Al₂O₃ ratio of USY zeolite. The average metal particle size was estimated to be in the range from 25 to 31 \AA , and was larger than the size of supercages of USY zeolites (13 \AA). Therefore, most of the Pd–Pt particles may exist on the external surface and in the bulk of USY with a local destruction of the zeolite framework, as suggested by Gallezot et al. [15].

The Fourier transforms of Pd K-edge EXAFS spectra of sulfided Pd–Pt/USY-10.7, Pd–Pt/USY-48, and Pd–Pt/USY-310 catalysts are shown in figure 1 (a), (b), and (c), respectively. The radial distance R from a Pd atom in figure 1 was shifted from the real bond distance due to a phase shift by potentials of adsorbing atoms and scattering atoms. The Pd–Pt/USY-10.7 catalyst showed peaks at $R = 1.88$ and 2.52 \AA (figure 1(a)). Unless the samples were sulfided, neither the calcined nor the reduced samples showed the peak at $R = 1.88$ \AA . When the EXAFS spectrum was simulated by FEFF calculation [16] for the PdS structure (Pd–S, 2.3 \AA) reported in the literature [17], the Pd–S peak appeared at 1.86 \AA , as shown in figure 1(d). On the other hand, the Pd–O peak for PdO appeared at 1.63 \AA [13]. In addition, the Pd–O peak appeared at 1.62 \AA for the Pd–Pt/HY-310 catalyst, which had been reduced and then deliberately exposed to air. Therefore, we assigned the peak at $R = 1.88$ \AA in figure 1(a) to the Pd–S bond, and not to the Pd–O bond. When the EXAFS spectrum of Pd-foil was measured, the Pd–Pd peak appeared at 2.48 \AA (figure 1(e)). The peak at $R = 2.52$ \AA in figure 1(a) was therefore in disagreement with the Pd–Pd peak. For Pd–Pt/NaY catalysts, Rades et al. [11] reported that the Pd–Pd peak splits into two peaks; one main peak at around 2.6 \AA and a shoulder peak at around 2.1 \AA , and that this main peak shifts from 2.52 to 2.67 \AA as the mol% of Pt increases from 0 to 75%. Similar observations were also reported by Toshima et al. [10] for polymer-protected Pd–Pt clusters. These two peaks arise from the phase interference effect of Pd–Pd and Pd–Pt, of which bond distances are almost the same [10,11]. Thus, the peak at $R = 2.52$ \AA in figure 1(a) would be generated by the phase interference effect for metallic Pd–Pd and Pd–Pt bonds. Both of the peaks due to the Pd–S and metallic Pd were also observed for the Pd–Pt/USY-48 and Pd–Pt/USY-310 catalysts (figure 1 (b) and (c), respectively).

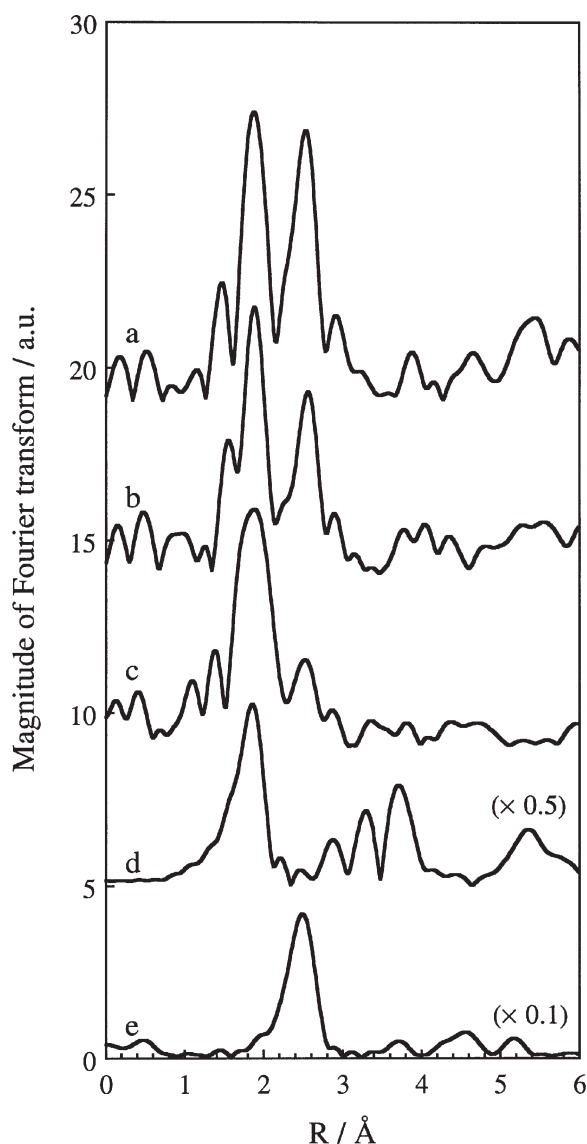


Figure 1. Fourier transforms of Pd K-edge EXAFS spectra for (a) sulfided Pd–Pt/USY-10.7 catalyst, (b) sulfided Pd–Pt/USY-48 catalyst, (c) sulfided Pd–Pt/USY-310 catalyst, (d) PdS simulated by FEFF calculation, and (e) Pd-foil.

As shown in figure 1, the height of the peak at $R = 2.52$ Å, evidence of metallic Pd–Pd and Pd–Pt bonds, significantly decreased with increasing $\text{SiO}_2/\text{Al}_2\text{O}_3$ ratio of USY. These results clearly indicate that the protection of Pd metal against sulfidation is the highest (i.e., highest sulfur tolerance) for the Pd–Pt/USY-10.7 catalyst and that this protection decreases (i.e., sulfur tolerance decreases) with increasing $\text{SiO}_2/\text{Al}_2\text{O}_3$ ratio. Only the Pd–S peak was observed for the Pd–Pt/ γ - Al_2O_3 catalyst sulfided under the same conditions, suggesting that sulfidation of Pd metal proceeds completely for the Pd–Pt/ γ - Al_2O_3 catalyst.

The Fourier transforms of Pt L_{III}-edge EXAFS spectra of sulfided Pd–Pt/USY-10.7, Pd–Pt/USY-48, and Pd–Pt/USY-310 catalysts are shown in figure 2 (a), (b), and (c), respectively. Similar to the Pd K-edge spectra (figure 1), the radial distance R from a Pt atom in figure 2 was shifted

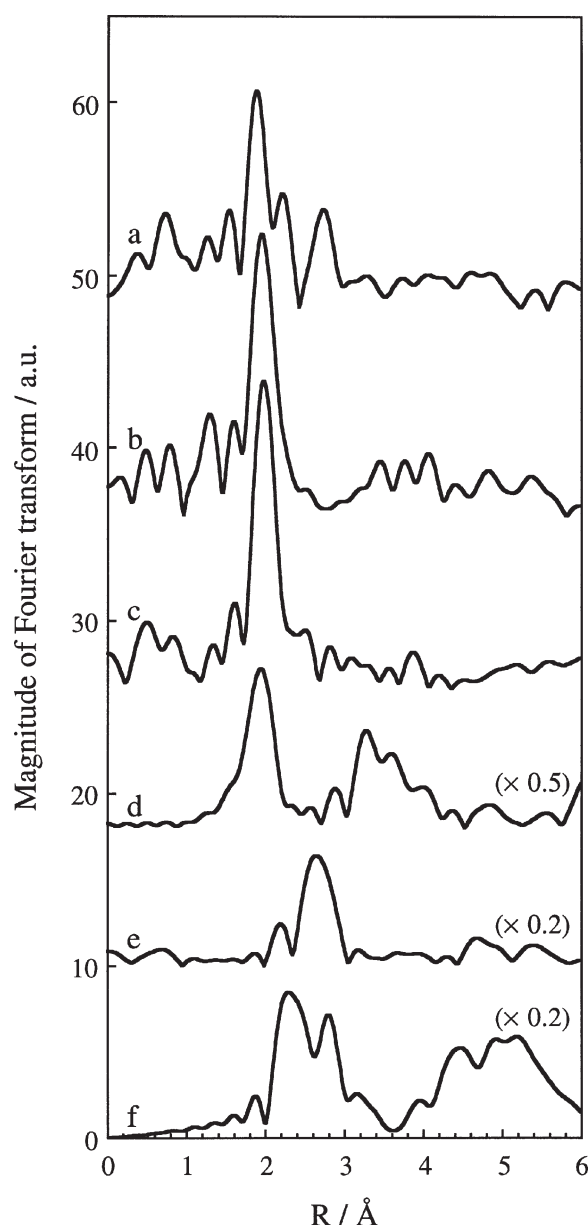


Figure 2. Fourier transforms of Pt L_{III}-edge EXAFS spectra for (a) sulfided Pd–Pt/USY-10.7 catalyst, (b) sulfided Pd–Pt/USY-48 catalyst, (c) sulfided Pd–Pt/USY-310 catalyst, (d) PtS simulated by FEFF calculation, (e) Pt-foil, and (f) simulated alloy structure of Pt and Pd (Pt: Pd = 1:1).

from the real bond distance by the phase shift. The Pd–Pt/USY-10.7 catalyst showed three peaks, at $R = 1.88$, 2.20 , and 2.72 Å (figure 2(a)), whereas the Pd–Pt/USY-48 and Pd–Pt/USY-310 catalysts showed only a single peak, at $R = 1.94$ Å (figure 2(b)) and 1.98 Å (figure 2(c)), respectively. The peaks at around $R = 1.94$ Å ($R = 1.88$ Å for Pd–Pt/USY-10.7, 1.94 Å for Pd–Pt/USY-48, and 1.98 Å for Pd–Pt/USY-310) shifted to a longer distance with increasing $\text{SiO}_2/\text{Al}_2\text{O}_3$ ratio. Unless the samples were sulfided, neither the calcined nor the reduced samples showed these peaks. FEFF simulation of the EXAFS spectrum for the PtS structure (Pt–S, 2.31 Å) reported in the literature [18] showed the Pt–S peak at 1.94 Å (figure 2(d)). In contrast, the Pt–O peak for PtO_2 appeared at 1.68 Å. In addition, the

Pt–O peak appeared at 1.64 Å for the Pd–Pt/HY-310 catalyst, which had been reduced and then deliberately exposed to air. Therefore, the peaks at $R = 1.88$ (Pd–Pt/USY-10.7), 1.94 (Pd–Pt/USY-48), and 1.98 Å (Pd–Pt/USY-310) would be assigned to the Pt–S bonds (not to the Pt–O bonds), although the bond distance slightly increased with increasing $\text{SiO}_2/\text{Al}_2\text{O}_3$ ratio. As shown in figure 2(e), the Pt–Pt peak for Pt-foil appeared at 2.68 Å. The peak at $R = 2.72$ Å (Pd–Pt/USY-10.7) in figure 2(a) was therefore in disagreement with the Pt–Pt peak. Figure 2(f) shows the Fourier transform of an average EXAFS spectrum of the spectrum for Pt metal and the spectrum for a Pt atom placed in the structure of Pd metal. The latter spectrum was simulated by FEFF calculation. Two peaks appeared, at around $R = 2.28$ and 2.80 Å, and similar to the peak at $R = 2.52$ Å in figure 1, were produced by the phase interference effect of Pt–Pt and Pt–Pd. Thus, the peaks at $R = 2.20$ and 2.72 Å for the Pd–Pt/USY-10.7 catalyst would be generated by the phase interference effect for metallic Pt–Pt and Pt–Pd bonds.

In addition to the Pt–S peak ($R = 1.88$ Å) (figure 2(a)), the peaks indicative of the existence of metallic Pt–Pt and Pt–Pd ($R = 2.20$ and 2.72 Å) remained in the Pd–Pt/USY-10.7 catalyst after sulfidation but completely disappeared in the Pd–Pt/USY-48 and Pd–Pt/USY-310 catalysts (figure 2 (b) and (c)). This indicates that Pt metal on the Pd–Pt/USY-10.7 catalyst survives sulfidation (i.e., high sulfur tolerance), whereas Pt on the Pd–Pt/USY-48 and Pd–Pt/USY-310 catalysts are easily sulfided (i.e., low sulfur tolerance). The sulfided Pd–Pt/ γ - Al_2O_3 catalyst showed only the Pt–S peak, suggesting that sulfidation of Pt metal as well as Pd metal proceeds completely for this catalyst.

The differences in the Fourier transforms of EXAFS spectra among the catalysts studied here clearly confirm for the first time that the sulfur tolerance of both Pd and Pt on USY-10.7 was the highest and then decreased with increasing $\text{SiO}_2/\text{Al}_2\text{O}_3$ ratio. The reason why the Pd–Pt/USY-10.7 catalyst had the highest sulfur tolerance can be explained as follows.

Adsorption of sulfur on a supported metal is affected by various parameters, such as the nature of the metal, the acidity of the support, or the metal dispersion. Sulfur preferentially adsorbs on sites of lowest coordination, such as corner and edge sites [19]. The number of such sites increases with decreasing particle size. For the catalysts that we studied, the average metal particle size slightly increased with increasing $\text{SiO}_2/\text{Al}_2\text{O}_3$ ratio (table 1). Therefore, the difference in the degree of sulfidation among the catalysts, that is, the decrease in the sulfur tolerance associated with an increase in the $\text{SiO}_2/\text{Al}_2\text{O}_3$ ratio, cannot be explained by a difference in the metal dispersion. When small metal crystallites are deposited on an acidic support, the metal becomes electron-deficient due to the interaction between the metal and acid sites. The metal thus becomes sulfur-tolerant because the bonding energy between the electron-deficient metal and the electron-acceptor sulfur is weakened [20–22]. The significance of this interaction effect will increase as the metal particle size decreases. We pre-

viously measured the acidity of USY zeolites by infrared spectroscopy of adsorbed pyridine, and reported that both the amount and strength of the Brønsted and Lewis acid sites decrease monotonically with increasing $\text{SiO}_2/\text{Al}_2\text{O}_3$ ratio when the ratio exceeds 10.7 [9]. This means that the acidity of USY-10.7 is higher than that of either USY-48 or USY-310. Therefore, the reason why the sulfur tolerance of Pd–Pt on USY-10.7 is the highest among the catalysts studied may be that adsorption of sulfur on Pd and Pt is suppressed by formation of the electron-deficient Pd–Pt particles caused by the interaction between Pd–Pt and the acid sites of USY-10.7.

Accordingly, the Pd–Pt/USY-10.7 catalyst potentially should be most active for the aromatic hydrogenation in the presence of sulfur compounds with respect to the sulfur tolerance. However, the hydrogenation activity of tetralin in the presence of dibenzothiophene for the Pd–Pt/USY-10.7 catalyst is lower than that for the Pd–Pt catalysts supported on USY zeolite, in which the $\text{SiO}_2/\text{Al}_2\text{O}_3$ ratio is in the range from 15 to 40 [9]. The reason for this low activity may be that USY-10.7 has few mesopores where the pore diffusional resistance of the reactant is relatively small, compared with USY zeolites whose $\text{SiO}_2/\text{Al}_2\text{O}_3$ ratio exceeds 15 [9]. The difference between Pd and Pt in the ease of sulfidation and the detailed structures of sulfided Pd–Pt bimetallic particles based on the coordination numbers are now under investigation.

4. Conclusions

Sulfur tolerance of bimetallic Pd–Pt (Pd : Pt mole ratio of 4 : 1) supported on USY zeolites ($\text{SiO}_2/\text{Al}_2\text{O}_3 = 10.7, 48$, and 310) was investigated using an EXAFS analysis. The results showed that (a) the highest sulfur tolerance for both Pd and Pt for the bimetallic Pd–Pt catalysts was achieved when Pd–Pt was supported on the highest-acidity USY zeolite ($\text{SiO}_2/\text{Al}_2\text{O}_3 = 10.7$), (b) the sulfur tolerance decreased with increasing $\text{SiO}_2/\text{Al}_2\text{O}_3$ ratio of the USY zeolites, that is, decreasing acidity of USY, and (c) the sulfur tolerance of Pd was higher than that of Pt for the Pd–Pt/USY ($\text{SiO}_2/\text{Al}_2\text{O}_3 = 48$ and 310) catalysts.

Acknowledgement

We thank Mr. M. Imamura and Dr. H. Shimada for the EXAFS measurements and for helpful discussions. We also thank Catalysts and Chemicals Industries Co. for the ICP measurements. The EXAFS work was done under the approval of the Photon Factory Program Advisory Committee.

References

- [1] A. Stanislaus and B.H. Cooper, Catal. Rev. Sci. Eng. 36 (1994) 75.
- [2] B.H. Cooper and B.B.L. Donniss, Appl. Catal. A 137 (1996) 203.
- [3] S.M. Kovach and G.D. Wilson, US Patent 3 943 053 (1974).

- [4] J.K. Minderhoud and J.P. Lucien, Eur. Patent 303 332 (1988).
- [5] S.G. Kukes, F.T. Clark, P.D. Hopkins and L.M. Green, US Patent 5 151 172 (1991).
- [6] T.-B. Lin, C.-A. Jan and J.-R. Chang, Ind. Eng. Chem. Res. 34 (1995) 4284.
- [7] C.-A. Jan, T.-B. Lin and J.-R. Chang, Ind. Eng. Chem. Res. 35 (1996) 3893.
- [8] H. Yasuda and Y. Yoshimura, Catal. Lett. 46 (1997) 43.
- [9] H. Yasuda, T. Sato and Y. Yoshimura, Catal. Today, in press.
- [10] N. Toshima, M. Harada, T. Yonezawa, K. Kushihashi and K. Asakura, J. Phys. Chem. 95 (1991) 7448.
- [11] T. Rades, C. Pak, M. Polisset-Thfoin, R. Ryoo and J. Fraissard, Catal. Lett. 29 (1994) 91.
- [12] P.L. Hansen, A.M. Molenbroek and A.V. Ruban, J. Phys. Chem. B 101 (1997) 1861.
- [13] N. Matsubayashi, H. Yasuda, M. Imamura and Y. Yoshimura, Catal. Today, in press.
- [14] J.R. Anderson, in: *Structure of Metallic Catalysts* (Academic Press, London, 1975) p. 296.
- [15] P. Gallezot, A. Alarcon-Diaz, J.A. Dalmon, A.J. Renouprez and B. Imelik, J. Catal. 39 (1975) 334.
- [16] J.J. Rehr, J. Mustre de Leon, S.I. Zabinsky and R.C. Albers, J. Am. Chem. Soc. 113 (1991) 5135.
- [17] T.F. Gaskell, Z. Krist. 96 (1937) 203.
- [18] F.A. Bannister and M.H. Hey, J. Mine. Soc. 23 (1932) 188.
- [19] J. Barbier, E. Lamy-Pitara, P. Marecot, J.P. Boitiaux, J. Cosyns and F. Verna, Adv. Catal. 37 (1990) 279.
- [20] R.A. Dalla Betta and M. Boudart, in: *Proc. 5th Int. Congr. on Catalysis*, Vol. 2 (North-Holland, Amsterdam, 1973) p. 1329.
- [21] P. Gallezot, Catal. Rev. Sci. Eng. 20 (1979) 121.
- [22] P. Gallezot and G. Bergeret, in: *Catalyst Deactivation*, eds. E.E. Petersen and A.T. Bell (Dekker, New York, 1987) p. 263.